Extracellular vesicles derived from mesenchymal stem cells suppress breast cancer progression by inhibiting angiogenesis

MANQIAN ZHOU[1,2*], HUIFANG LI[2*], JINGLEI ZHAO[2*], QIAONAN ZHANG[2], ZHIBO HAN[3-5], ZHONG-CHAO HAN[3-5], LIHONG ZHU[6], HUI WANG[1] and ZONGJIN LI[2,7,8]

[1]Department of Radiation Oncology, Tianjin Union Medical Center, Nankai University, Tianjin 300121, P.R. China; [2]School of Medicine, Nankai University, Tianjin 300071, P.R. China; [3]Jiangxi Engineering Research Center for Stem Cell, Health & Biotech Co., Shangrao, Jiangxi 334001, P.R. China; [4]Tianjin Key Laboratory of Engineering Technologies for Cell Pharmaceutical, National Engineering Research Center for Cell Products, AmCellGene Co., Ltd., Tianjin 300457, P.R. China; [5]Beijing Engineering Laboratory of Perinatal Stem Cells, Beijing Institute of Health and Stem Cells, Health & Biotech Co., Beijing 100176, P.R. China; [6]Department of Gynecologic Oncology, Beijing Obstetrics and Gynecology Hospital, Capital Medical University, Beijing 100026, P.R. China; [7]Tianjin Key Laboratory of Human Development and Reproductive Regulation, Tianjin Central Hospital of Gynecology Obstetrics, Nankai University Affiliated Hospital of Obstetrics and Gynecology, Tianjin 300052, P.R. China; [8]National Key Laboratory of Kidney Diseases, Chinese PLA General Hospital, Beijing 100853, P.R. China

Received December 22, 2023; Accepted July 19, 2024

DOI: 10.3892/mmr.2024.13316

Abstract. Previous studies have highlighted the antitumor effects of mesenchymal stem cell-derived extracellular vesicles (MSC-EVs), positioning them as a promising therapeutic avenue for cancer treatment. However, some researchers have proposed a bidirectional influence of MSC-EVs on tumors, determined by the specific tissue origin of the MSCs and the types of tumors involved. The present study aimed to elucidate the effects of human placenta MSC-derived extracellular vesicles (hPMSC-EVs) on the malignant behavior of a mouse breast cancer model of 4T1 cells *in vitro* and *in vivo*. The findings revealed that hPMSC-EVs significantly inhibited the proliferation, migration and colony formation of cultured 4T1 mouse breast cancer cells without inducing apoptosis. Exposure to conditioned medium from 4T1 cells pretreated with hPMSC-EVs resulted in decreased angiogenic activity, accompanied by the downregulation of angiogenesis-promoting genes in human umbilical vein endothelial cells. In murine xenograft models derived from the 4T1 cell line, local administration of hPMSC-EVs substantially hindered tumor growth. Further results revealed that hPMSC-EVs inhibited angiogenesis *in vivo*, as reflected by the use of a vascular growth factor receptor 2-Fluc transgenic mouse model. In summary, the results confirmed that hPMSC-EVs negatively modulated breast cancer growth by suppressing tumor cell proliferation and migration via an indirect antiangiogenic mechanism. These results underscored the therapeutic potential of EVs, suggesting a promising avenue for alternative anticancer treatments in the future.

Correspondence to: Professor Zongjin Li, School of Medicine, Nankai University, 94 Weijin Road, Tianjin 300071, P.R. China
E-mail: zongjinli@nankai.edu.cn

*Contributed equally

Key words: extracellular vesicles, mesenchymal stem cells, breast cancer, angiogenesis

Introduction

Mesenchymal stem cells (MSCs) have been widely studied for their potential applications in various medical fields, including regenerative medicine and cancer therapy (1-4). MSCs are multipotent stromal cells that can differentiate into a variety of cell types, including bone cells, cartilage cells and adipose cells. They also possess immunomodulatory properties, making them attractive candidates for therapeutic applications (5). The potential of MSCs in cancer treatment is an area of active research, but the outcomes and involved mechanisms are complex and can vary depending on several factors, including the type of cancer, the microenvironment and the specific characteristics of the MSCs used (6). Studies have suggested that MSCs can promote tumor growth and metastasis under certain conditions (7). The supportive roles of MSCs in the tumor microenvironment may be related to their interactions with cancer cells, immune cells and the extracellular matrix. However, some research suggests that MSCs may exert antitumor effects (8,9). They may inhibit cancer cell growth through mechanisms such as inducing apoptosis (programmed cell death) or modulating immune responses to target cancer cells (7,10).

Extracellular vesicles (EVs) carry various bioactive molecules, including proteins, nucleic acids and lipids. They are involved in cell-to-cell communication and have been frequently investigated for potential therapeutic applications (11). MSC-derived EVs (MSC-EVs) are a heterogeneous

group of lipid-coated nanovesicles that mainly serve as paracrine mediators of MSCs. Equipped with the characteristics of MSCs, MSC-EVs show a strong tendency to migrate to tumor sites *in vivo* and as anticancer therapeutic candidates, they are considered superior to MSCs in a number of ways, such as being cell-free and tiny, nonimmunogenic, easy to manipulate, and biologically genetically safe (12). A number of studies have shown that MSC-EVs are involved in tumor regulation by affecting various steps of tumor growth and metastasis through positive or negative mechanisms (12-14). It seems that whether MSC-EVs promote or suppress tumor progression is determined by the origin of the MSC and the type of tumor (6). The potential anticancer effects of EVs derived from mesenchymal stem cells on various types of cancer are unclear.

Breast cancer is the most prevalent cancer type and the leading cause of cancer-related mortality among women (15,16). Despite the improvements in cancer treatment throughout recent decades, a large percentage of patients still experience disappointing results. New creative approaches that can increase the effectiveness of treatment are urgently needed. As aforementioned, the physiological roles of EVs derived from mesenchymal stem cells in cancer are unclear. The human placenta, a temporary vascular organ that occurs during fetal development, has emerged as an alternative and highly attractive source of MSCs and MSC-released EVs (17). Therefore, the potent effects of EVs derived from human placenta mesenchymal stem cells (hPMSC-EVs) on breast cancer progression were validated in the present study and it demonstrated that hPMSC-EVs can inhibit the proliferation, migration and colony formation of the 4T1 breast cancer cell line, decrease the tube formation potential of human umbilical vein endothelial cells (HUVECs) *in vitro*, and inhibit tumor growth and angiogenesis in models derived from the 4T1 cell line.

Materials and methods

Cell culture. The mouse breast cancer cell line 4T1 was purchased from ATCC and cultured in RPMI 1640 medium supplemented with 10% FBS (cat. no. SV30087.02; HyClone; Cytiva), 1% penicillin-streptomycin solution (cat. no. 15140122; Gibco; Thermo Fisher Scientific, Inc.) and 1% nonessential amino acid solution (cat. no. 11140050; Gibco; Thermo Fisher Scientific, Inc.). The human breast cancer cell line MCF-7 was purchased from ATCC and cultured in Dulbecco's modified Eagle's medium (DMEM; cat. no. 11995065; Gibco; Thermo Fisher Scientific, Inc.) supplemented with 10% FBS and 1% penicillin-streptomycin solution (cat. no. 15140122; Gibco; Thermo Fisher Scientific, Inc.). HUVECs (passage 3-4), human placenta-derived MSCs (hPMSCs; passage 4-6) and human umbilical cord-derived MSCs (hUC-MSCs; passage 4-6) were donated by AmCellGene Co. Ltd. and preserved at Nankai University (18). For the tracking of transplanted tumor cells *in vivo*, 4T1 cells were transduced with a self-activating lentiviral vector that carried a 5'LTR promoter-driven double fusion (DF) reporter gene that contained firefly luciferase and enhanced green fluorescence protein (Fluc-eGFP) as previously reported (19,20).

Isolation and characterization of EVs. EVs were isolated by ultracentrifugation as previously described (11,18). The supernatant of MSCs was successively centrifuged at 500 x g for 10 min, 2,000 x g for 30 min and 10,000 x g for 30 min at 4˚C to exclude cell debris and apoptotic bodies. After that, the EV pellet was collected by ultracentrifugation at 100,000 x g for 70 min and washed by a second ultracentrifugation at 100,000 x g for 2 h in phosphate-buffered saline (PBS). All the above ultracentrifugation steps were performed at 4˚C. Finally, the purified EV pellet was resuspended in 200 μl PBS and stored at -80˚C for further experiments. Transmission electron microscopy (TEM; HT7700; Hitachi, Ltd.) was used to observe the morphology of the isolated EVs (18). Briefly, 2 μg/μl EVs were loaded onto a carbon film (Zhongjingkeyi Technology), incubated for 5 min at room temperature and was subsequently stained with 2% phosphotungstic acid for 2 min at room temperature. Excess liquid was removed by filter paper. The samples were allowed to air dry for at least 10 min at room temperature and then observed using TEM at an acceleration voltage of 120 kV. The size distribution of EVs was determined using a Malvern Particle Size Analyzer (Zeta sizer Nano ZS; Malvern Instruments, Ltd.). The protein concentration was quantified using a BCA protein assay kit (Promega Corporation).

Western blotting. In the present study, the proteins expressed in MSCs and MSC-EVs, including tumor susceptibility gene 101 (TSG101), ALG-2 interacting protein X (ALIX) and CD63, were identified as previously reported (21). In brief, 30 μg of EVs lysates in 100 μl radioimmunoprecipitation assay (RIPA) buffer (cat. no. R0010; Beijing Solarbio Science & Technology Co., Ltd.), determined by BCA protein assay kit (Promega Corporation), were subjected to western blotting analysis. Proteins were heat-denaturized in 5X SDS-PAGE loading buffer (cat. no. CW0027S; CWBIO), fractionated on 10% SDS-polyacrylamide gels, and electro-transferred onto polyvinylidene fluoride membranes (MilliporeSigma). Blocked with 5% non-fat milk (cat. no. A600669; Beyotime Institute of Biotechnology) for 2 h at room temperature, proteins were respectively immunoblotted with the indicated antibodies. Briefly, they were incubated with primary antibodies at 4˚C overnight and subsequently identified by second antibodies through a second incubation step of 2 h at room temperature. The following antibodies were used according to the manufacturer's instructions: ALIX (1:2,000; cat. no. WL03063; Wanleibio Co., Ltd.), TSG101 (1:2,000; cat. no. EPR7131; Abcam) and CD63 (1:2,000; cat. no. WL02549; Wanleibio Co., Ltd.). The secondary antibody applied in this study was HRP-labeled Goat Anti-Rabbit IgG (H+L; 1:1,000; cat. no. A0208; Beyotime Institute of Biotechnology). The blot bands were visualized with enhanced chemiluminescence detection reagent (cat. no. WP20005; Thermo Fisher Scientific, Inc.) and analyzed by ImageJ software (version 1.54j; National Institutes of Health).

Cell apoptosis and proliferation analysis. To determine whether hPMSC-EVs could induce apoptosis in 4T1 cells, Annexin V/propidium iodide (PI) fluorescence-activated cell sorting (FACS) analysis was performed with a FACS instrument (FACSCalibur; BD Biosciences). Single-cell suspension of 4T1 cells was harvested after 24 h of EV treatment and stained using an Annexin V/PI kit (cat. no. CA1040; Beijing

Solarbio Science & Technology Co., Ltd.) to assess the apoptotic proportion of 4T1 cells. According to the manufacturer's protocol, 100 μl of 4T1 cell suspension at a concentration of 1-5x10^6/ml was firstly stained with 5 μl Annexin V for 5 min at room temperature. Then, 5 μl PI (20 μg/ml) and 400 μl phosphate-buffered saline (PBS) were added and detected immediately. The PBS-treated 4T1 cells were used as control, and the Annexin V^-/PI^- cells were identified as live cells. The Annexin V^+/PI^- cells were identified as early apoptotic cells, Annexin V^+/PI^+ cells were identified as late apoptotic cells, and Annexin V^-/PI^+ cells were scored as necrotic cells. Data were analyzed by FlowJo 10 (FlowJo LLC). To investigate whether hPMSC-EVs affect cell proliferation, 4T1 cells were treated with hPMSC-EVs and evaluated by bioluminescence imaging.

Collection of conditioned medium (CM). For the collection of 4T1 CM, 4T1 cells were primitively cultured in 1640 medium. When the confluence reached 40%, the old medium was replaced with a fresh complete medium supplemented with 5 mg EVs. After 48 h, the supernatants were harvested and stored at -80˚C. For the collection of HUVEC-CM, which served as a control in the present study, the complete HUVEC medium was replaced with 7 ml of EGM-2 per T25 flask (Corning, Inc.), with HUVECs also reaching 40% confluence. After 48 h, the supernatants were collected and stored at -80˚C.

Cell migration assay. Transwell assays were performed using Transwell chambers through a filter membrane with the pore size of 8 μm (MilliporeSigma). Briefly, 1x10^5 Fluc-GFP-labeled 4T1 cells immersed in 200 μl of RPMI 1640 medium supplemented with 2% FBS were seeded in the upper inserts. RPMI 1640 supplemented with 10% FBS was added to the lower chamber. The low concentration of FBS in the upper inserts prevents cell proliferation, consistent with previous reports (22). After 24 h, non-migrated cells on the upper side of the filter were removed with a cotton swab. The migrated cells were counted under a confocal microscope at a magnification of 200x and five randomly chosen fields were selected for each insert. The experiments were repeated at least three times. For the wound healing assay, cells were seeded in 6-well plates at a density of 2x10^5 per well and grown to 90% confluence. Sterile 10 μl tips (Corning Life Sciences) were used to create 2-3 straight wounds in each well, followed by medium replacement and treatment with 100 μg/ml EV. In this assay, similar to the Transwell assay, 10% FBS from RPMI 1640 was replaced with 2% low-concentration FBS to suppress 4T1 cell proliferation. The images were captured and reported temporally, with an interval of 12 h. The number of cells that migrated to the wound area was calculated using ImageJ software (Version 1.54j; National Institutes of Health).

Tube formation assay. HUVECs treated with hPMSC-EVs were subjected to a tube formation assay. In brief, precooled Matrigel (BD Biosciences) was pipetted into a 48-well plate, which was maintained at 4˚C overnight. Before the HUVECs were seeded in Matrigel-treated 48-well plates, they were placed in an incubator and rewarmed to 37˚C. Afterwards, the HUVECs were seeded into 48-well plates at a density of 5x10^4 cells/well, which were randomly divided into two groups and cultured with EGM-2 medium. In particular, CM from 4T1 cells treated with hPMSC-EVs was added to the medium of HUVECs in the EV group. After culturing for 6 h, tube formation was observed under a microscope (ECLIPSE Ti-U; Nikon Corporation); five fields were chosen randomly and analyzed using ImageJ software (Version 1.54j; National Institutes of Health).

Colony formation assay. 4T1 cells were seeded into a six-well plate at 1,000 cells per well and subsequently treated with hPMSC-EVs at a concentration of 100 μg/ml and an equal volume of PBS was also repeatedly added to the control group every other day. After two weeks, the cells were washed with PBS and then stained with crystal violet and the colonies with more than 50 cells were counted and analyzed.

Animal model. In the present study, 12 BALB/c mice (female, 8-12 weeks old) were purchased from Biocytogen. To monitor the angiogenic effects of EVs *in vivo* in real time, transgenic mice expressing firefly luciferase under the promoter of VEGFR2 (VEGFR2-luc) were obtained from Xenogen Corporation. All experimental procedures were conducted according to institutional guidelines for the Care and Use of Laboratory Animals at Nankai University, Tianjin, China (23) and in accordance with the National Institutes of Health (NIH) Guide for the Care and Use of Laboratory Animals, 8th edition (24). The mice were housed in a specific pathogen-free environment, the temperature and humidity of which were maintained at 21-23˚C and 45-50%, respectively. With a 12-h light/dark cycle (lights on 07:00-19:00 h), the housing facility supplied the mice with sufficient food and water. The 4T1-derived xenograft model was established according to the following protocol. Mice were anesthetized with isoflurane, 2.0% induction for 4 min, 1.5% maintenance and 1l/min oxygen inhalation (19). For the animal model of the 4T1-derived xenograft model, BALB/c mice were inoculated with 1x10^6 4T1 (Fluc-eGFP) cells in the fourth pair of mammary fat pads. Once the tumors were palpable, which could be judged after ~4 days of tumor inoculation (day 0), the mice were randomly divided into two groups (six mice per group).

In the experimental group, 100 μg of MSC-EVs were peri-injected into the tumors on days 0, 2 and 4. In the control group, a peritumoral injection of PBS was administered on days 0, 2 and 4. All mice were observed for tumor progression and treatment effects by BLI for up to 14 days prior to sacrifice and tumor tissues from the two groups were collected for histological analysis. Under the same conditions, the VEGFR2-luc mice were inoculated with unlabeled 4T1 cells (15,25) and BLI was also performed on days 0, 4, 7, 10 and 14. On day 14, mice were sacrificed by cervical dislocation. The tumors were removed for further histological analysis. The humane endpoints (e.g., severe distress, inability to eat or drink, significant weight loss, behavioral abnormalities indicating suffering) were used to determine whether animals should be sacrificed before the end of the study.

In vivo BLI. BLI was performed in all experimental mice at specific time points using the IVIS Lumina imaging system (Xenogen Corporation). Fluc imaging of DF-labeled 4T1 cells was performed to observe tumor progression and metastasis and assess the therapeutic effects of hPMSC-EVs. For angiogenesis experiments in VEGFR2 transgenic mice,

Fluc imaging was used to visualize VEGFR2 expression. Mice were anesthetized with isoflurane, 2.0% induction for 4 min, 1.5% maintenance and 1l/min oxygen inhalation (19). After intraperitoneal injections of reporter probe D-Luciferin (150 mg of luciferin/kg), animals were imaged for 2 sec to 2 min. The BLI signal was quantified by the average radiance of the region of interest over the xenograft tumor using Living Image Software (version 4.7; PerkinElmer, Inc.) (15,25).

Immunofluorescence staining. Immunofluorescence staining was performed on frozen sections of 4T1 xenograft tumor samples to detect neovasculature in 4T1 tumor tissue. Sections were incubated with primary antibodies against CD31 (1:200; cat. no. 550274; BD Biosciences), Ki67 (1:200; cat. no. 571599; BD Biosciences) for 2 h at room temperature, followed by incubation with Alexa Fluor 594-labeled secondary antibodies (1:500; cat. no. A21209; Invitrogen; Thermo Fisher Scientific, Inc.) for 30 min at room temperature. The nuclei were stained with DAPI for 5 min at room temperature. Fluorescence images (magnification, x200) were acquired with a microscope (FV1000; Olympus Corporation) and analyzed with ImageJ software (Version 1.54j; National Institutes of Health).

Reverse transcription-quantitative (RT-q) PCR. To assess the mRNA expression levels of the analyzed genes, total RNA was extracted from HUVECs at a confluence of 80-90% and tumor tissues treated with TRIzol® reagent (cat. no. 15596018CN; Thermo Fisher Scientific, Inc.) according to the manufacturer's protocol. First-strand cDNA was synthesized using reverse transcriptase-mediated oligo-dT primers (cat. no. 11151ES60; Yeasen Biotech). Subsequently, RT-qPCR was performed on an Opticon System (Bio-Rad Laboratories, Inc.) in 20 μl reaction volumes. The level of mRNA expression was quantified using the TransStart Top Green qPCR SuperMix Kit (cat. no. AQ131-01; TransGen Biotech Co., Ltd.). The $2^{-\Delta\Delta Cq}$ method was used to determine the relative changes in mRNA folding (26). The primers and amplification conditions are listed in the Tables SI and SII.

Statistical analysis. All experiments were performed in triplicate for each condition and repeated at least three times. The data are presented as the means ± standard deviations (SDs). For comparisons between two groups, two-tailed paired Student's t-tests were performed. For comparisons among multiple groups, one-way ANOVA followed by the least significant difference post hoc test was used. $P<0.05$ was considered to indicate a statistically significant difference.

Results

Characterization of hPMSC-derived EVs (hPMSC-EVs). The phenotype of hPMSCs was confirmed by surface marker expression via FACS analysis (Fig. S1). EVs were isolated from the supernatant of hPMSCs by ultracentrifugation and then characterized by TEM, nanoparticle tracking analysis (NTA) and western blotting. The enriched particles exhibited a typical cup-shaped morphology under TEM (Fig. 1A) and relatively heterogeneous sizes of ~120 nm in diameter (Fig. 1B). Western blot analysis confirmed the expression of classical EV markers (TSG101, ALIX and CD63) in hPMSC-EVs (Figs. 1C and S2), which is consistent with a previous report (20).

hPMSCs-EVs inhibit cell proliferation but not apoptosis. A recent study reported that MSCs and their EVs can be tumorigenic or antitumorigenic by affecting multiple steps of tumor progression (6). To determine the effects of hPMSC-EVs on breast cancer, 4T1 cells were labeled with an Fluc-GFP double fusion reporter gene (Fig. S3) and apoptosis and proliferation were assessed after treatment with MSC-EVs. Annexin V and PI FACS analysis was performed (Fig. 2A), which revealed that hPMSC-EV treatment did not induce apoptosis in cultured 4T1 cells; however, changes in cell morphology, the elongation of some cells with filamentous ends and a decrease in cell number, were detected via brightfield microscopy, indicating that cell status was adversely affected by EV treatment (Fig. 2B). The morphology of 4T1 cells induced by EVs needs to be clarified to exclude the possibility that it is induced by cell-cell contact. Under identical experimental conditions, control group exhibited rapid 4T1 cell proliferation and increased cell-cell contact. According to the results, the effect of cell-cell contacts during proliferation tended to make the cells more tightly packed. The proportion of cells with elongated, filamentous ends was significantly higher in the EV group compared with the control group. The EV group exhibited significantly lower cell density and confluence compared with the control group, suggesting a diminished role of cell-cell contact in influencing 4T1 cell morphology. In summary, the morphological changes in 4T1 cells may be the result of both cell-cell contact and EV treatment and the role of EVs may be the primary factor involved. Concurrently, the hPMSC-EV-mediated suppression of the proliferation of other breast cancer cells, such as MCF-7 cells, was also validated. Consistent results were revealed using EVs from human umbilical cord MSCs (hUCMSCs), which validated the universality of the present study (Figs. S4 and S5). Furthermore, under BLI, EV treatment led to a significantly reduced Fluc signal, indicating that cell viability was decreased and that cellular proliferation was inhibited (Fig. 2C and D).

CM from hPMSC-EV-treated 4T1 cells weakens the angiogenic potential of HUVECs. Angiogenesis is the basis for solid tumor growth and metastasis. Blocking the formation of new blood vessels in solid tumors has proven to be a highly efficient anticancer strategy. The present study explored the effects of hPMSC-EVs on tumor angiogenesis using HUVECs, a widely used model system for researches related to tumor vascular biology. First, the supernatant of 4T1 cells that had been pretreated with EV for 24 h was collected as CM. Then, a wound healing assay was performed in HUVECs and the results showed that 4T1-CM led to decreased cell motility in HUVECs (Fig. 3A and B). Similarly, the Ki-67 immunofluorescence assay showed that 4T1-CM reduced the number of proliferating endothelial cells (Fig. 3C and D). In addition, Matrigel was used to detect the tube formation of endothelial cells. By counting nodes and junctions, it was found that 4T1-CM treatment markedly reduced HUVEC tube formation (Fig. 3E and F). Furthermore, RT-qPCR revealed that the expression of angiogenesis-related genes (VEGFA, VEGFR2, Ang-1, Ang-2, b-FGF, HIF-1α and PDGF) was significantly downregulated in HUVECs following 4T1-CM treatment (Fig. 3G). These results indicated that hPMSC-EVs can indirectly reduce the neovasculature of 4T1 tumors.

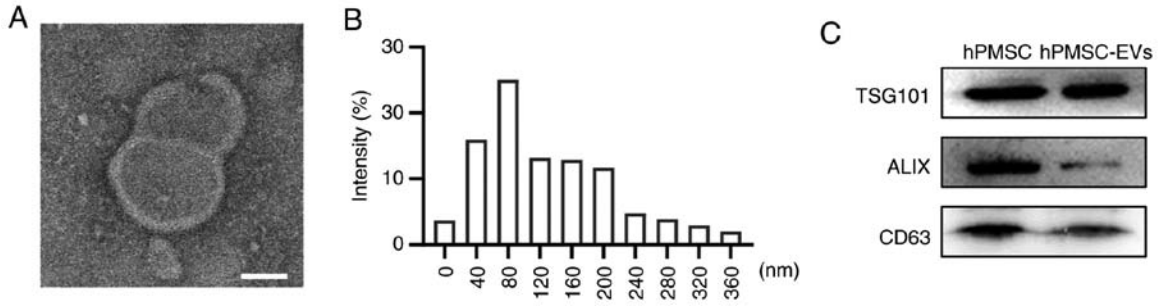

Figure 1. Characterization of hPMSC-EVs. (A) Representative TEM image of isolated EVs. Scale bar, 50 nm. (B) Size distribution of EVs measured by NTA. (C) Western blot analysis of the expression of the EV-specific biomarkers CD63, ALIX and TSG101 in isolated MSC-EVs. Uncropped immunoblots can be found in Fig. S2. hPMSC-EVs, human placenta MSC-derived extracellular vesicles; TEM, transmission electron microscopy; NTA, nanoparticle tracking analysis; EVs, extracellular vesicles.

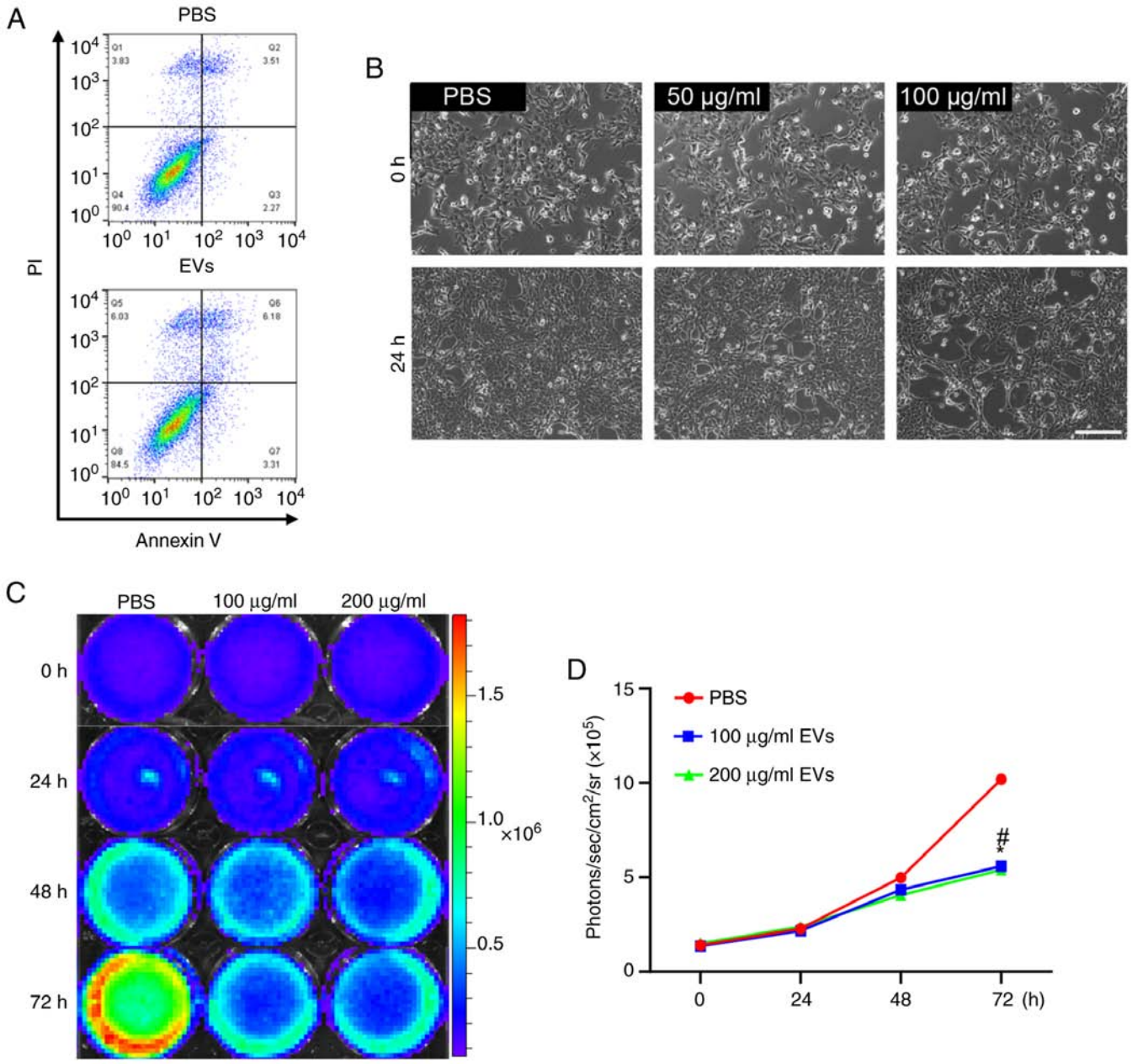

Figure 2. hPMSC-EVs do not induce apoptosis in 4T1 cells but decreased cell proliferation. (A) Fluorescence-activated cell sorting staining with Annexin V/propidium iodide was performed to detect apoptotic 4T1 cells following hPMSC-EV treatment. (B) The effects of EVs on the morphology of 4T1 cells were observed using bright-field microscopy. Scale bar, 100 μm. (C) Bioluminescence imaging showed decreasing Fluc signals in 4T1 cells at 24, 48 and 72 h after EV treatment. (D) Quantitative analysis of imaging signals. n=3, $^{\#}$P<0.05 100 μg/ml EVs vs. PBS, *P<0.05 200 μg/ml EVs vs. PBS. hPMSC-EVs, human placenta MSC-derived extracellular vesicles; EVs, extracellular vesicles.

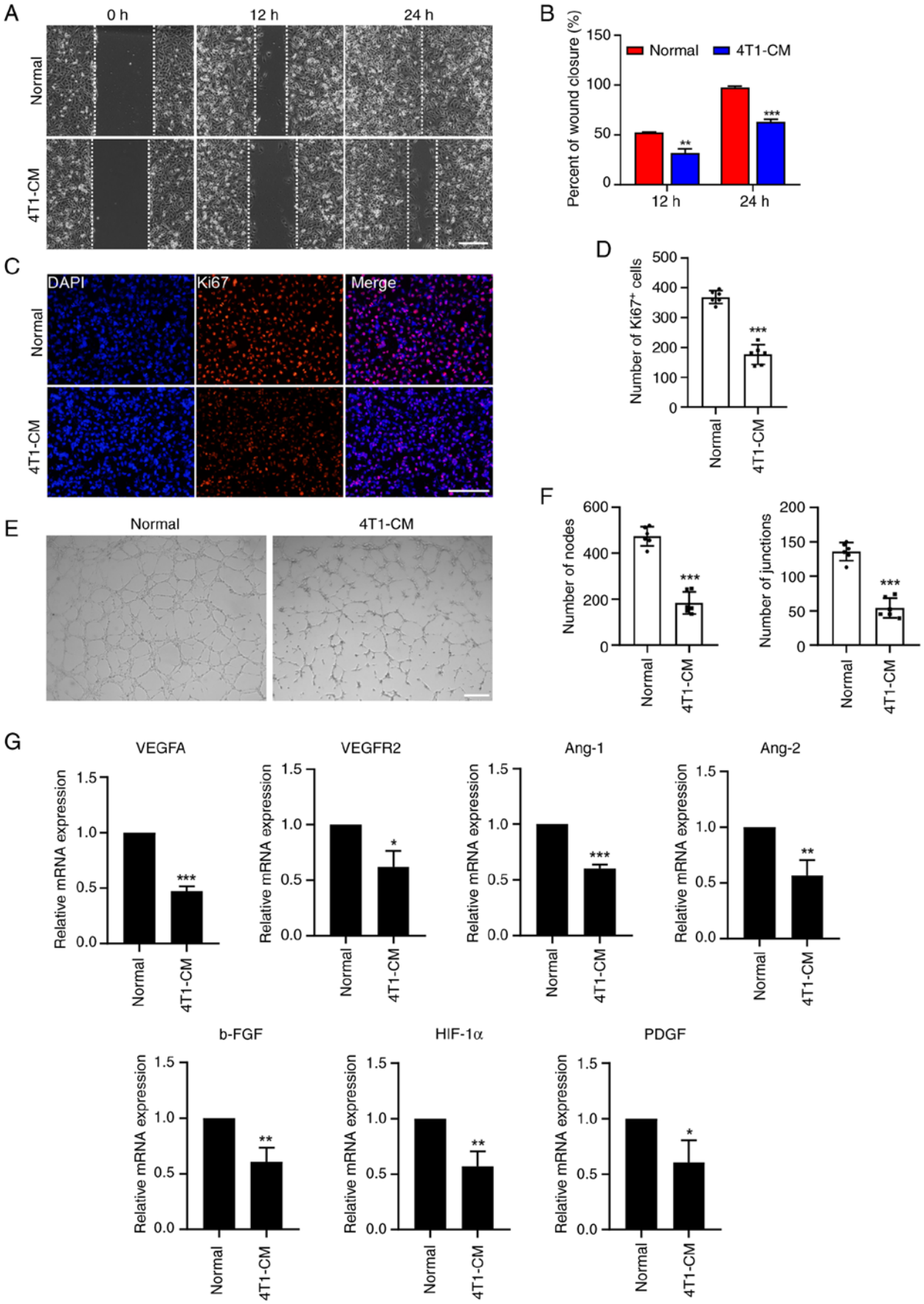

Figure 3. Effects of 4T1-CM on HUVEC angiogenesis observed *in vitro*. (A) Representative images of the wound healing assay of HUVECs treated with 4T1-CM. Scale bar, 100 μm. (B) The wound healing area per field decreased following treatment with HUVECs and 4T1-CM. (C) Representative immunofluorescence images of Ki-67 (red) expression in HUVECs. Scale bar, 100 μm. (D) Percentages of Ki67-positive cells. (E) Optical images of tube formation by HUVECs. Scale bar, 100 μm. (F) Quantitative evaluation of nodes and junctions using ImageJ software. (G) Reverse transcription-quantitative PCR analysis of angiogenic gene expression in HUVECs treated with 4T1-CM. n=3, *P<0.05, **P<0.01, ***P<0.001. HUVECs, human umbilical vein endothelial cells.

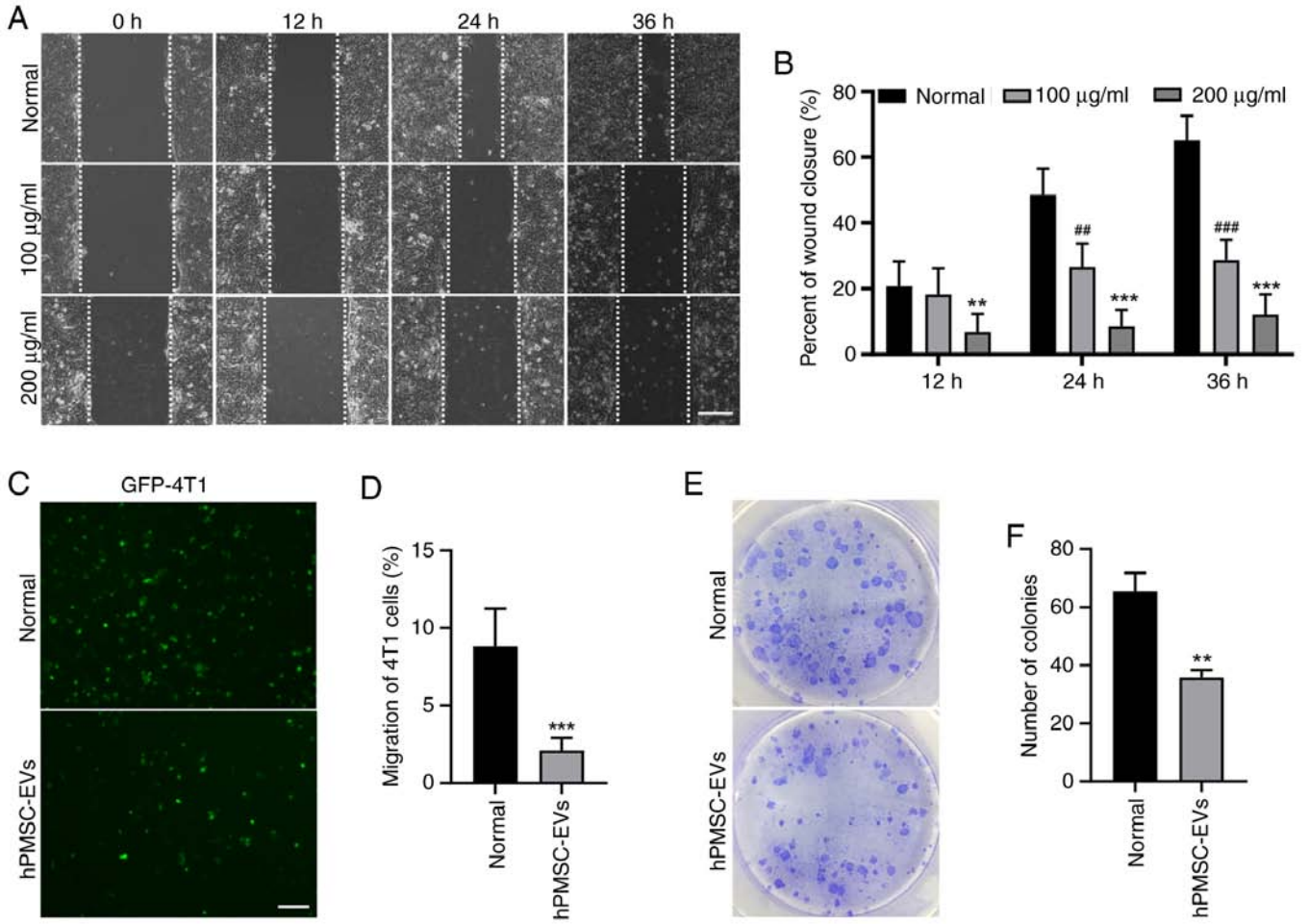

Figure 4. hPMSC-EVs inhibited 4T1 cell migration and colony formation *in vitro*. (A) Representative images of the wound healing assay of 4T1 cells treated with 100/200 μg/ml EVs. Scale bar, 100 μm. (B) The wound healing area per field was reduced following EV treatment. n=3, $^{\#\#}$P<0.01, $^{\#\#\#}$P<0.001, 100 μg/ml EVs vs. normal group, **P<0.01, ***P<0.001, 200 μg/ml EVs vs. normal group. (C) Transwell assays showed that 4T1 cell migration was reduced after treatment with 100 μg/ml EV. Scale bar, 200 μm. (D) Number of migratory cells calculated using ImageJ software. ***P<0.001. (E and F) The effects of EVs on the independent viability of 4T1 cells, as shown by colony formation experiments. n=3, **P<0.01. hPMSC-EVs, human placenta MSC-derived extracellular vesicles; EVs, extracellular vesicles.

hPMSC-EVs reduced 4T1 cell migration and colony formation. Tumor metastasis occurs when tumor cells migrate from one site to another and stably proliferate. The migration and colony formation abilities of tumor cells indicate a metastatic phenotype, which is closely related to a poor prognosis. The results of the present study revealed that, according to the wound healing assay, 4T1 cell migration was significantly suppressed by EV treatment (Fig. 4A and B). Consistent results were obtained in the Transwell assay, showing a decrease in the migration of GFP-labeled 4T1 cells (Fig. 4C and D). The colony formation assay also revealed decreased colony formation after EV treatment (Fig. 4E and F). These findings suggested that hPMSC-derived EVs may suppress the migration of 4T1 breast cancer cells.

hPMSC-EVs suppress tumor growth. As the aforementioned assays revealed that hPMSCs-EVs could inhibit the growth and migration of 4T1 cells *in vitro*, the present study next performed *in vivo* studies for further verification by BLI. A murine model of breast cancer was established by subcutaneously transplanting 10^6 Fluc/GFP-labeled 4T1 cells into BALB/c mice. BLI showed that the number of tumor cells was reduced and that tumor progression was inhibited by the local administration of hPMSC-derived EVs (Fig. 5A and B). The mice were sacrificed 14 days following hPMSC-EV treatment and the tumors were harvested. Morphologically, the tumors in the EV treatment group were smaller than those in the control group (Fig. 5C). This finding was verified by further statistical analysis of tumor volume and weight (Fig. 5D and E). Furthermore, immunofluorescence staining of the Ki67 protein, a classical tumor cell proliferation marker, revealed a significant decrease in the number of cells in the proliferating state and the quantification analysis also showed an identical trend (Fig. 5F and G). No toxicity of hPMSCs-EVs was observed and all animals reached endpoints of the present study.

hPMSCs-EVs suppress angiogenesis in 4T1 breast tumors. VEGFR2-Fluc transgenic mice were subjected to angiogenesis observation via BLI at tumor sites. After hPMSC-EVs were administered, there was a dramatic decrease in VEGFR2 expression (Fig. 6A and B). CD31 immunofluorescence staining was performed after the mice were sacrificed and the tumors were removed, showing that EV treatment led to a reduction in the number of new blood vessels at the tumor sites (Fig. 6C).

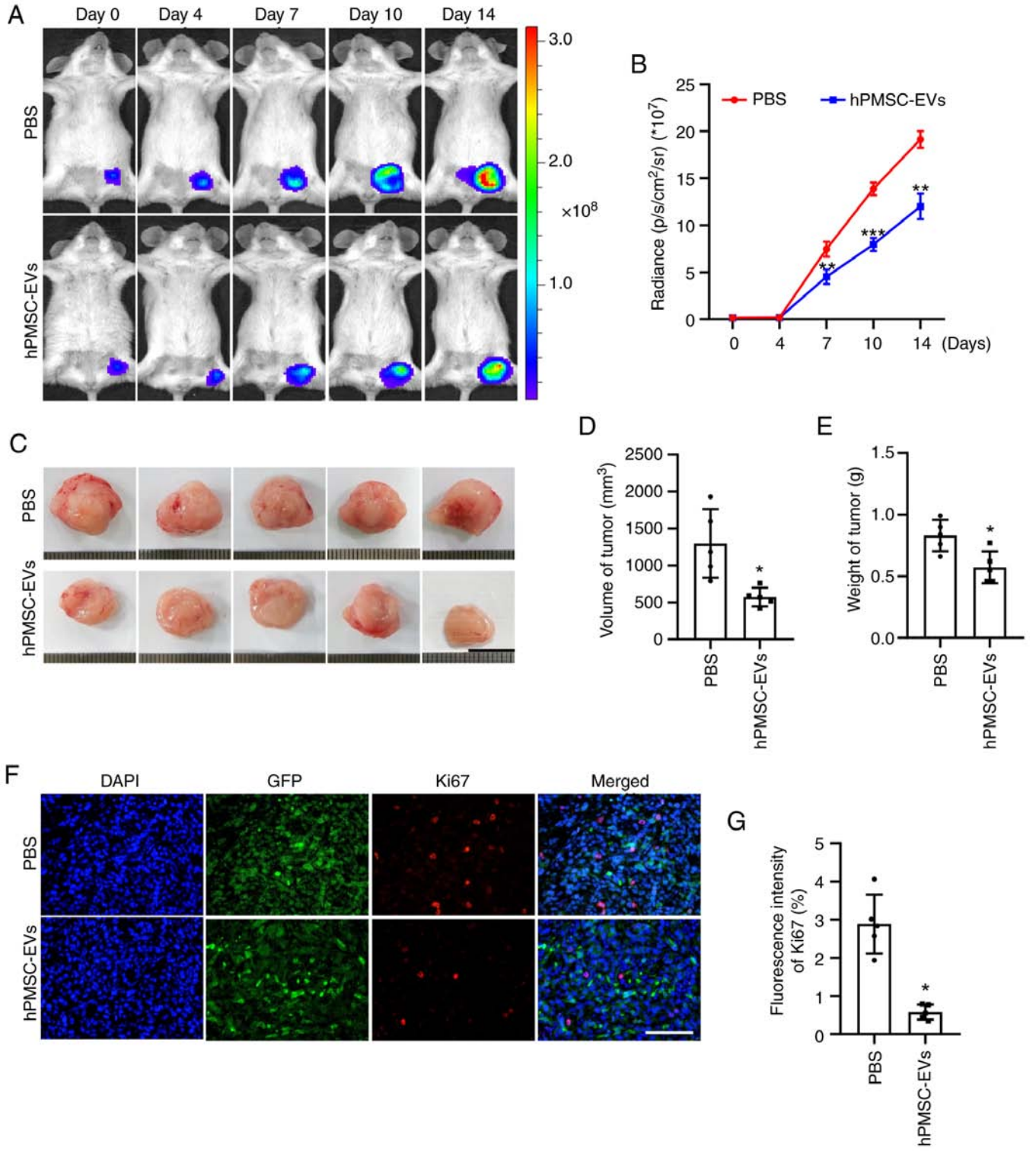

Figure 5. Inhibitory effect of hPMSC-EVs on tumor growth *in vivo*. (A) Firefly luciferase (Fluc) imaging of tumor growth. Representative animals were injected with $1x10^6$ 4T1 cells (Fluc/GFP). (B) Quantitative analysis of the Fluc signal, n=3. (C) Representative images of tumors isolated from sacrificed mice after 14 days of EV treatment. Scale bar, 1 cm. Quantitative analysis of tumor (D) volume and (E) weight, n=5. (F) Representative image of Ki-67 immunofluorescence staining in 4T1 cells. Scale bar, 100 μm. (G) Quantitative analysis of Ki-67 expression in 4T1 cells. n=5, PBS, *P<0.05, **P<0.01, ***P<0.001 vs. PBS. hPMSC-EVs, human placenta MSC-derived extracellular vesicles; EVs, extracellular vesicles.

Then, RNA was extracted from tumor tissues and RT-qPCR revealed that the expression of the angiogenesis-related genes, VEGFA, Ang-1, Ang-2, b-FGF, and PDGF, was significantly downregulated at tumor sites (Fig. 6D). These results indicated that MSC-EVs suppressed angiogenesis in 4T1 breast tumors.

Discussion

MSC-EVs have been identified as crucial paracrine regulators in a number of physiological and pathological processes (5). With a strong tendency to migrate to injury and tumor sites

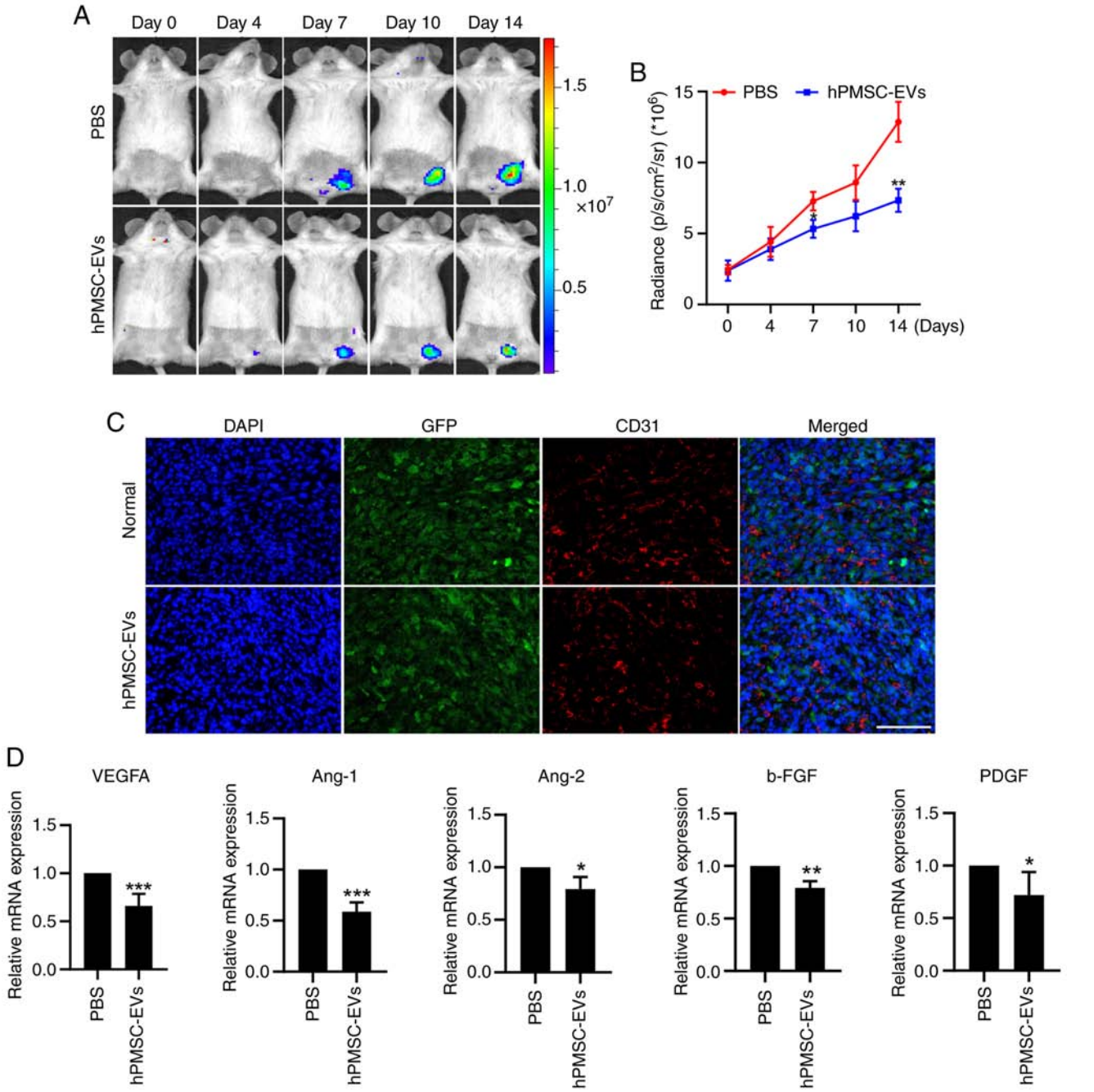

Figure 6. hPMSC-derived EVs inhibit 4T1 tumor angiogenesis *in vivo*. (A) *In vivo* monitoring of VEGFR2-luc expression following the transplantation of 4T1 cells into VEGFR2-Fluc transgenic mice with or without hPMSC-EV treatment. (B) Quantitative analysis of the dynamic trend of angiogenesis via Fluc signals, n=3. (C) Representative immunofluorescence images of CD31 in tumors harvested from sacrificed mice. Scale bar, 100 μm. (D) Reverse transcription-quantitative PCR analysis of angiogenic gene expression in tumor tissues treated with EVs, n=3, *P<0.05, **P<0.01, ***P<0.001 vs. PBS. hPMSC-EVs, human placenta MSC-derived extracellular vesicles; EVs, extracellular vesicles.

in vivo, MSC-EVs hold great promise as cell-free therapeutic approaches for a variety of medical conditions (27,28). However, the effects of MSC-EVs on tumor development and progression remain controversial (6,29). Some studies have shown proliferative effects, while others have demonstrated inhibitory effects of MSC-EVs on tumors (30,31). This difference in function could be attributed to the different tissue origins of MSCs and tumor types. The placenta is a neonatal-related proliferative tissue, usually discarded after fetal birth, in which MSCs are abundant. Placenta-derived MSCs are more proliferative, with an extended cell cycle and greater differentiation potential. Notably, compared with that of other MSCs, the wider antitumor effect of MSCs is hypothesized to be associated with the ability of the placenta to filter out harmful substances in the bloodstream of the mother (31,32). Therefore, placenta-derived MSC-EVs can act as candidates for antitumor therapies (7,33,34).

The present study revealed that human placenta-derived MSC-EVs had strong antitumor effects on 4T1 breast cancer models both *in vitro* and *in vivo*. hPMSC-EVs decreased the proliferation, migration and colony formation of cultured 4T1 cells but did not induce cell apoptosis. The angiogenic

potential of HUVECs was also weakened following exposure to CM from 4T1 cells pretreated with hPMSC-EVs. In 4T1 tumor-bearing mouse models, systemic administration of hPMSC-EVs resulted in impaired tumor growth, decreased vascularization and downregulated expression of angiogenesis-related genes. These findings indicated that hPMSC-EVs are antitumorigenic and may be good candidates for therapeutic alternatives for the treatment of breast cancer (35).

The tumor neovasculature is crucial for maintaining the survival and growth of solid tumors (35). MSC-EVs have been reported to modulate tumor vascularization in a positive or negative manner, similar to their bidirectional effect on tumor progression (36). The present study revealed that hPMSC-EVs inhibited tumor neovasculature, which may indicate that EVs, which contain abundant active cargoes, modify the function of 4T1 cells and lead to decreased release of proangiogenic factors. The major active components in hPMSC-EVs responsible for the antitumor effects need to be elucidated. On the one hand, the delayed tumor progression observed in the present study was attributed to multiple factors, including the reduced proliferation of 4T1 breast cancer cells, the weakened migration and tube formation ability of HUVECs and decreased angiogenesis. This pathological phenomenon, as a direct or indirect result of hPMSC-EV effects on 4T1 cells or breast cancer cells, is associated with several mechanisms. However, the inducers that lead to the occurrence of the aforementioned pathological phenomenon may be numerous and not completely identical. The results of the present study supported the diversity and complexity of the biological components of hPMSC-EVs. The cargo carried by EVs, including DNA, RNA, miRNA and other molecules, is abundant. Therefore, by combining the multiple medical effects of hPMSC-EVs on 4T1-based breast cancer cells and the complexity of the active factors contained in EVs, the anticancer effect of hPMSC-EVs may be exerted through the synergetic interaction of numerous active factors. As mentioned in the introduction, the potential applications of MSCs in cancer treatment are an area of active research and the outcomes and mechanisms involved are complex and can vary depending on several factors, including the type of cancer, the microenvironment and the specific characteristics of the MSCs used. Thus, the interaction between EVs and the microenvironment of the cancer nest may be one of the major factors that boosts the anticancer effect. In conclusion, multiple factors may be involved in the anticancer effect of hPMSC-EVs, the synergetic interaction of which commonly suppresses breast cancer progression. Furthermore, compared with the absence of apoptosis, female menstruation is a highly important angiogenic process in organs related to pregnancy and this regulation could also be extended to stromal cells and cell products, which seems to support the notable antiangiogenic effect of hPMSC-EVs, as observed in the present study.

The present study, is the first to report, to the best of the authors' knowledge, that non-modified hPMSC-EVs acted as antitumor agents for 4T1-derived breast cancer and to reveal several mechanisms related to their actions. 4T1 represents a triple-negative, highly malignant murine breast cancer cell line that is normally used for standardized animal models of human breast cancer. MCF-7, MDA-231 and other human-derived breast cancer cell lines that need an immune suppressor environment to grow into xenograft tumors, may lead to unreliable results because MSC-EVs are also deeply involved in the process of immune regulation by nature, while the 4T1 cell line can avoid these concerns, as it can grow in immunocompetent rodents.

In summary, the present study explored the effects of hPMSC-EVs on 4T1 breast cancer cells and revealed that tumor cell growth could be suppressed both *in vitro* and *in vivo* by inhibiting cellular proliferation and tumor angiogenesis. This significant finding indicated that if reproducible in humans, hPMSC-EVs could be clinically exploited for their antitumor potential and could represent a promising strategy for the treatment of breast cancer.

Acknowledgements

Not applicable.

Funding

The present study was partially supported by the Tianjin Natural Science Foundation (grant nos. 22JCZXJC00170 and 21JCZDJC00070), Open Funding from the Nankai University Eye Institute (grant no. NKYKD202203) and the Tianjin Key Medical Discipline (Specialty) Construction Project (grant no. TJYXZDXK-043A).

Availability of data and materials

The data generated in the present study are included in the figures and/or tables of this article.

Authors' contributions

HW and ZL were responsible for conceptualization. MZ, HL, JZ and QZ were responsible for the acquisition of data. MZ, HL and LZ were responsible for formal analysis. HW and ZJ were responsible for methodology. ZL and LZ were responsible for project administration and supervision. ZH and ZCH were responsible for validation and visualization. MZ and HL wrote the original draft of the manuscript and ZL and LZ reviewed and edited the manuscript. MZ, HL and ZL confirmed the authenticity of all the raw data. All authors read and approved the final manuscript.

Ethics approval and consent to participate

The Ethics Committee for the Use of Animals of Nankai University approved the experimental protocols for studies of EVs for cancer therapy (approval no. 20210022; date of approval: February 23, 2021).

Patient consent for publication

Not applicable.

Competing interests

The authors declare that they have no competing interests. AmCellGene Co., Ltd. had no commercial interest in the present study.

References

1. Al-Awsi GRL, Alsaikhan F, Margiana R, Ahmad I, Patra I, Najm MAA, Yasin G, Rasulova I, Hammid AT, Kzar HH, *et al*: Shining the light on mesenchymal stem cell-derived exosomes in breast cancer. Stem Cell Res Ther 14: 21, 2023.
2. Wan W, Miao Y, Niu Y, Zhu K, Ma Y, Pan M, Ma B and Wei Q: Human umbilical cord mesenchymal stem cells conditioned medium exerts anti-tumor effects on KGN cells in a cell density-dependent manner through activation of the Hippo pathway. Stem Cell Res Ther 14: 46, 2023.
3. Bae J, Liu L, Moore C, Hsu E, Zhang A, Ren Z, Sun Z, Wang X, Zhu J, Shen J, *et al*: IL-2 delivery by engineered mesenchymal stem cells re-invigorates $CD8^+$ T cells to overcome immunotherapy resistance in cancer. Nat Cell Biol 24: 1754-1765, 2022.
4. Chen F, Zhong X, Dai Q, Li K, Zhang W, Wang J, Zhao Y, Shen J, Xiao Z, Xing H and Li J: Human umbilical cord MSC delivered-soluble TRAIL inhibits the proliferation and promotes apoptosis of B-ALL cell in vitro and in vivo. Pharmaceuticals (Basel) 15: 1391, 2022.
5. Zhou X, Zhang W, Liu Y, Zhang L and Li Z: Chapter 5-Mesenchymal stem cells: A promising weapon for cancer therapy. In: Zhang L, Han Z, Wang J, Li Z and Huang Q (eds). Mesenchymal Stem Cells. Academic Press, pp119-141, 2023.
6. Wang J, Ma Y, Long Y and Chen Y: Extracellular vesicle derived from mesenchymal stem cells have bidirectional effects on the development of lung cancer. Front Oncol 12: 914832, 2022.
7. Eiro N, Fraile M, Fernández-Francos S, Sánchez R, Costa LA and Vizoso FJ: Importance of the origin of mesenchymal (stem) stromal cells in cancer biology: 'Alliance' or 'war' in intercellular signals. Cell Biosci 11: 109, 2021.
8. Ma Z, Xie W, Luo T, Hu Z, Hua J, Zhou J, Yang T, Wang W, Song Z, Yu X, *et al*: Exosomes from TNF-α preconditioned human umbilical cord mesenchymal stromal cells inhibit the autophagy of acinar cells of severe acute pancreatitis via shuttling bioactive metabolites. Cell Mol Life Sci 80: 257, 2023.
9. Lee MW, Ryu S, Kim DS, Lee JW, Sung KW, Koo HH and Yoo KH: Mesenchymal stem cells in suppression or progression of hematologic malignancy: Current status and challenges. Leukemia 33: 597-611, 2019.
10. Xia C, Wang T, Cheng H, Dong Y, Weng Q, Sun G, Zhou P, Wang K, Liu X, Geng Y, *et al*: Mesenchymal stem cells suppress leukemia via macrophage-mediated functional restoration of bone marrow microenvironment. Leukemia 34: 2375-2383, 2020.
11. Li R, Wang C, Zhou M, Liu Y, Chen S, Chai Z, Huang H, Zhang K, Han Z, Hua G, *et al*: Heparan sulfate proteoglycan-mediated internalization of extracellular vesicles ameliorates liver fibrosis by targeting hepatic stellate cells. Extracellul Vesicle 1: 100018, 2022.
12. Zhao J, Lin H and Huang K: Mesenchymal stem cell-derived extracellular vesicles transmitting MicroRNA-34a-5p suppress tumorigenesis of colorectal cancer through c-MYC/DNMT3a/PTEN axis. Mol Neurobiol 59: 47-60, 2022.
13. You B, Jin C, Zhang J, Xu M, Xu W, Sun Z and Qian H: MSC-derived extracellular vesicle-delivered L-PGDS inhibit gastric cancer progression by suppressing cancer cell stemness and STAT3 phosphorylation. Stem Cells Int 2022: 9668239, 2022.
14. Yang S, Wang L, Gu L, Wang Z, Wang Y, Wang J and Zhang Y: Mesenchymal stem cell-derived extracellular vesicles alleviate cervical cancer by delivering microRNA-331-3p to reduce LIM zinc finger domain containing 2 methylation in tumor cells. Hum Mol Genet 31: 3829-3845, 2022.
15. Su W, Wang L, Zhou M, Liu Z, Hu S, Tong L, Liu Y, Fan Y, Kong D, Zheng Y, *et al*: Human embryonic stem cell-derived endothelial cells as cellular delivery vehicles for treatment of metastatic breast cancer. Cell Transplant 22: 2079-2090, 2013.
16. Arnold M, Morgan E, Rumgay H, Mafra A, Singh D, Laversanne M, Vignat J, Gralow JR, Cardoso F, Siesling S and Soerjomataram I: Current and future burden of breast cancer: Global statistics for 2020 and 2040. Breast 66: 15-23, 2022.
17. Li Z and Han ZC: Introduction of perinatal tissue-derived stem cells. In: Han ZC, Takahashi TA, Han Z and Li Z (eds). Perinatal Stem Cells: Biology, Manufacturing and Translational Medicine. Singapore: Springer Singapore, pp1-7, 2019.
18. Zhang K, Li R, Chen X, Yan H, Li H, Zhao X, Huang H, Chen S, Liu Y, Wang K, *et al*: Renal endothelial cell-targeted extracellular vesicles protect the kidney from ischemic injury. Adv Sci (Weinh) 10: e2204626, 2023.
19. Hezam K, Wang C, Fu E, Zhou M, Liu Y, Wang H, Zhu L, Han Z, Han ZC, Chang Y and Li Z: Superior protective effects of PGE2 priming mesenchymal stem cells against LPS-induced acute lung injury (ALI) through macrophage immunomodulation. Stem Cell Res Ther 14: 48, 2023.
20. Jia P, Zhao X, Liu Y, Liu M, Zhang Q, Chen S, Huang H, Jia Y, Chang Y, Chen S, *et al*: The RGD-modified self-assembling D-form peptide hydrogel enhances the therapeutic effects of mesenchymal stem cells (MSC) for hindlimb ischemia by promoting angiogenesis. Chem Eng J 450: 138004, 2022.
21. Li H, Huang H, Chen X, Chen S, Yu L, Wang C, Liu Y, Zhang K, Wu L, Han ZC, *et al*: The delivery of hsa-miR-11401 by extracellular vesicles can relieve doxorubicin-induced mesenchymal stem cell apoptosis. Stem Cell Res Ther 12: 77, 2021.
22. Zhang K, Zhao X, Chen X, Wei Y, Du W, Wang Y, Liu L, Zhao W, Han Z, Kong D, *et al*: Enhanced therapeutic effects of mesenchymal stem cell-derived exosomes with an injectable hydrogel for hindlimb ischemia treatment. ACS Appl Mater Interfaces 10: 30081-30091, 2018.
23. Wang C, Hezam K, Fu E, Pan K, Liu Y and Li Z: In vivo tracking of mesenchymal stem cell dynamics and therapeutics in LPS-induced acute lung injury models. Exp Cell Res 437: 114013, 2024.
24. National Research Council (US) Committee for the Update of the Guide for the Care and Use of Laboratory Animals: The National Academies Collection: Reports funded by National Institutes of Health. Guide for the Care and Use of Laboratory Animals. 8th edition. Washington (DC): National Academies Press (US). Copyright © 2011, National Academy of Sciences, 2011.
25. Zhou M, Wang L, Su W, Tong L, Liu Y, Fan Y, Luo N, Zheng Y, Zhao H, Xiang R and Li Z: Assessment of therapeutic efficacy of liposomal nanoparticles mediated gene delivery by molecular imaging for cancer therapy. J Biomed Nanotechnol 8: 742-750, 2012.
26. Livak KJ and Schmittgen TD: Analysis of relative gene expression data using real-time quantitative PCR and the 2(-Delta Delta C(T)) method. Methods 25: 402-408, 2001.
27. Moradi-Chaleshtori M, Bandehpour M, Heidari N, Mohammadi-Yeganeh S and Mahmoud Hashemi S: Exosome-mediated miR-33 transfer induces M1 polarization in mouse macrophages and exerts antitumor effect in 4T1 breast cancer cell line. Int Immunopharmacol 90: 107198, 2021.
28. Wang M, Li J, Wang D, Xin Y and Liu Z: The effects of mesenchymal stem cells on the chemotherapy of colorectal cancer. Biomed Pharmacother 160: 114373, 2023.
29. Hong IS, Lee HY and Kang KS: Mesenchymal stem cells and cancer: Friends or enemies? Mutat Res 768: 98-106, 2014.
30. Rahimi Tesiye M, Abrishami Kia Z and Rajabi-Maham H: Mesenchymal stem cells and prostate cancer: A concise review of therapeutic potentials and biological aspects. Stem Cell Res 63: 102864, 2022.
31. Zhao Y, Shen M, Wu L, Yang H, Yao Y, Yang Q, Du J, Liu L, Li Y and Bai Y: Stromal cells in the tumor microenvironment: Accomplices of tumor progression? Cell Death Dis 14: 587, 2023.
32. Li T, Zhang C, Ding Y, Zhai W, Liu K, Bu F, Tu T, Sun L, Zhu W, Zhou F, *et al*: Umbilical cord-derived mesenchymal stem cells promote proliferation and migration in MCF-7 and MDA-MB-231 breast cancer cells through activation of the ERK pathway. Oncol Rep 34: 1469-1477, 2015.
33. Du L, Tao X and Shen X: Human umbilical cord mesenchymal stem cell-derived exosomes inhibit migration and invasion of breast cancer cells via miR-21-5p/ZNF367 pathway. Breast Cancer 28: 829-837, 2021.
34. Bailey AJM, Tieu A, Gupta M, Slobodian M, Shorr R, Ramsay T, Rodriguez RA, Fergusson DA, Lalu MM and Allan DS: Mesenchymal stromal cell-derived extracellular vesicles in preclinical animal models of tumor growth: Systematic review and meta-analysis. Stem Cell Rev Rep 18: 993-1006, 2022.
35. Aravindhan S, Ejam SS, Lafta MH, Markov A, Yumashev AV and Ahmadi M: Mesenchymal stem cells and cancer therapy: Insights into targeting the tumour vasculature. Cancer Cell Int 21: 158, 2021.
36. Luo T, von der Ohe J and Hass R: MSC-Derived extracellular vesicles in tumors and therapy. Cancers (Basel) 13: 5212, 2021.